

1 First report of genetic transformation and CRISPR/Cas12a- 2 mediated gene editing of European beech (*Fagus sylvatica* L.)

3 Virginia Zahn, Alice-Jeannine Sievers, Birgit Kersten, Matthias Fladung, Tobias Bruegmann*

4

5 Affiliation:

6 Thünen Institute of Forest Genetics, Sieker Landstrasse 2, D-22927 Grosshansdorf, Germany

7 *) tobias.bruegmann@thuenen.de, tobias.bruegmann@tobiology.de

8

9 Keywords:

10 Genome editing, CRISPR/Cas, *ttLbCas12a*, PEG-mediated transformation, protoplast isolation, *PDS*,
11 forest tree, promoter test

12

13 ORCIDs:

14 VZ: <https://orcid.org/0009-0001-1473-9311>

15 BK: <https://orcid.org/0000-0001-9900-9133>

16 MF: <https://orcid.org/0000-0001-9301-8581>

17 TB: <https://orcid.org/0000-0001-9823-5630>

18

19 Abstract

20 *Fagus sylvatica* L. (European beech) is a dominant hardwood forest tree species across Central Europe,
21 supporting diverse ecosystem services and forming the basis of a significant market for high-value
22 timber. However, climate change increasingly threatens beech vitality and productivity, making
23 molecular insights into its stress resilience and functional validation of underlying genes urgently
24 needed. Here, we report an improved protocol for protoplast isolation from seedling leaves and
25 demonstrate, for the first time, transient genetic transformation and CRISPR/Cas-mediated genome
26 editing in *F. sylvatica*. PEG-mediated transformation was sequentially optimized, achieving efficiencies
27 of $59 \pm 6.19\%$. Transformation efficiency was strongly influenced by season, which also affected
28 protoplast yield. Both, a basic molecular toolkit for functional genomics and future biotechnological
29 applications were established by testing a set of promoters and reporters. For proof-of-concept genome

30 editing, we achieved 4.75 to 32.69% editing efficiencies in the *PHYTOENE DESATURASE* gene
31 (*FsPDS*) using temperature-tolerant *LbCas12a* (*ttLbCas12a*). The establishment of a reliable protoplast
32 transformation and editing system provides a crucial foundation for future genetic improvement and
33 functional studies in this non-model tree species.

34 Introduction

35 European beech (*Fagus sylvatica* L.), beech for short, is one of the most widespread deciduous tree
36 species in Central Europe, forming stable climax stands across broad latitudinal and longitudinal
37 gradients (Fuchs et al., 2024; Houston Durrant et al., 2016). Combining ecological and economic values,
38 beech has become a cornerstone of near-natural, climate-resilient forestry in Central Europe (Felton et
39 al., 2010; Wühlisch, 2008). However, beech is increasingly threatened by climate change, as evidenced
40 by widespread crown defoliation (Bussotti et al., 2024; Corcobado et al., 2020; Langer and Bußkamp,
41 2023), affecting 82% of German beech in 2024 (BMLEH, 2025). In Germany alone, the economic loss
42 caused by the decline of beech trees is projected to range from €180 billion up to €4 trillion, depending
43 on the scenario (Baumbach et al., 2019). Understanding the molecular basis of climate resilience in
44 beech has thus become an urgent research priority (Cuervo-Alarcon et al., 2018; Pfenninger et al.,
45 2021).

46 Forest trees lag far behind annual crops in the application of molecular tools (Borthakur et al., 2022).
47 Tree breeding remains predominantly phenotypic and gene function studies via transgenic approaches
48 are nascent even in the model tree genus *Populus* (Sulis et al., 2023; Zhou et al., 2024b). This gap is
49 compounded by long generation times (approx. 50 years in beech; (Houston Durrant et al., 2016), large
50 heterozygous genomes lacking robust reference assemblies, and recalcitrance to *in vitro* regeneration
51 (An et al., 2020; Cao et al., 2022; Wang et al., 2025; Zahn et al., 2025). Although a high-quality reference
52 genome for beech has recently become available, its gene models still lack the depth of experimental
53 validation (Mishra et al., 2021).

54 Protoplasts—single plant cells whose cell wall has been enzymatically degraded—enable rapid,
55 regeneration-independent functional assays at the cell level (Tan et al., 2013; Yoo et al., 2007). PEG-
56 mediated protoplast transformation is the most widely used method for DNA uptake, allowing direct
57 testing of gene constructs, including promoter-reporter assays or guide RNAs for genome editing (Dai
58 et al., 2021; Panda et al., 2024; Wang et al., 2021). This approach is especially valuable for beech,
59 whose high recalcitrance to *in vitro* culture and whole-plant regeneration has been recognized since the
60 late 1970s and continues to engage current research (Chalupa, 1979; Thiesen et al., 2025; Zahn et al.,
61 2025). When combined with plant regeneration, protoplast-based systems enable DNA-free genome
62 editing via ribonucleoprotein delivery, which is considered particularly advantageous in the context of
63 regulatory frameworks and public acceptance (Marques et al., 2025; Tuncel et al., 2025). Earlier
64 protocols were limited to the isolation of protoplasts from freshly emerged leaves of field-grown trees
65 (Ahuja, 1984; Lang and Kohlenbach, 1988). To date, protoplast transformation has not been reported

66 for beech, despite its efficient application in many other forest tree species (Chen et al., 2025; Lu et al.,
67 2025; Pavese et al., 2024).

68 CRISPR/Cas-mediated gene editing has revolutionized functional genomics across diverse plant
69 species (Jinek et al., 2012; Mao et al., 2013; Wang et al., 2017; Zetsche et al., 2015). Among forest
70 trees, the use of CRISPR/Cas12a was only reported in initial studies in poplar (An et al., 2020; Das et
71 al., 2025; Li et al., 2023; Zhang et al., 2023). Compared to the commonly used Cas9, Cas12a offers
72 advantages such as recognizing a T-rich protospacer-adjacent motif (PAM) sequence, producing
73 staggered DNA cuts, and requiring a shorter guide RNA (crRNA) (Zetsche et al., 2015). We employed
74 the temperature-tolerant *ttLbCas12a* variant, which enhances editing efficiency at the lower
75 temperatures typical of plant tissue culture (Malzahn et al., 2019; Merker et al., 2020; Schindele and
76 Puchta, 2020). Multiple crRNAs were selected based on predicted secondary structure to maximize
77 editing efficiency (Creutzburg et al., 2020; Zhu and Liang, 2019). The *PHYTOENE DESATURASE* gene
78 (*PDS*) was identified in beech and subsequently used as the target gene. *PDS* encodes a key enzyme
79 in the carotenoid biosynthesis pathway that is frequently used as a model editing locus due to its
80 potential for visual phenotypes and ease of identification due to high sequence conservation (An et al.,
81 2020; Fan et al., 2015; Hirschberg, 2001; Mao et al., 2013; Pavese et al., 2021; Walawage et al., 2019).

82 Here, we first present a protocol for efficient protoplast isolation from beech seedling leaves with high
83 yield and vitality. We then report the first successful transient transformation in beech, systematically
84 optimizing key parameters of PEG-mediated DNA uptake. As a step towards building a molecular
85 toolbox for beech, we successfully demonstrated the functionality of a panel of constitutive promoters
86 driving the expression of fluorescent proteins. Finally, using *ttLbCas12a* and four crRNAs, we achieved
87 nucleotide deletions in the *FsPDS* gene, marking the first successful genome editing in European beech.

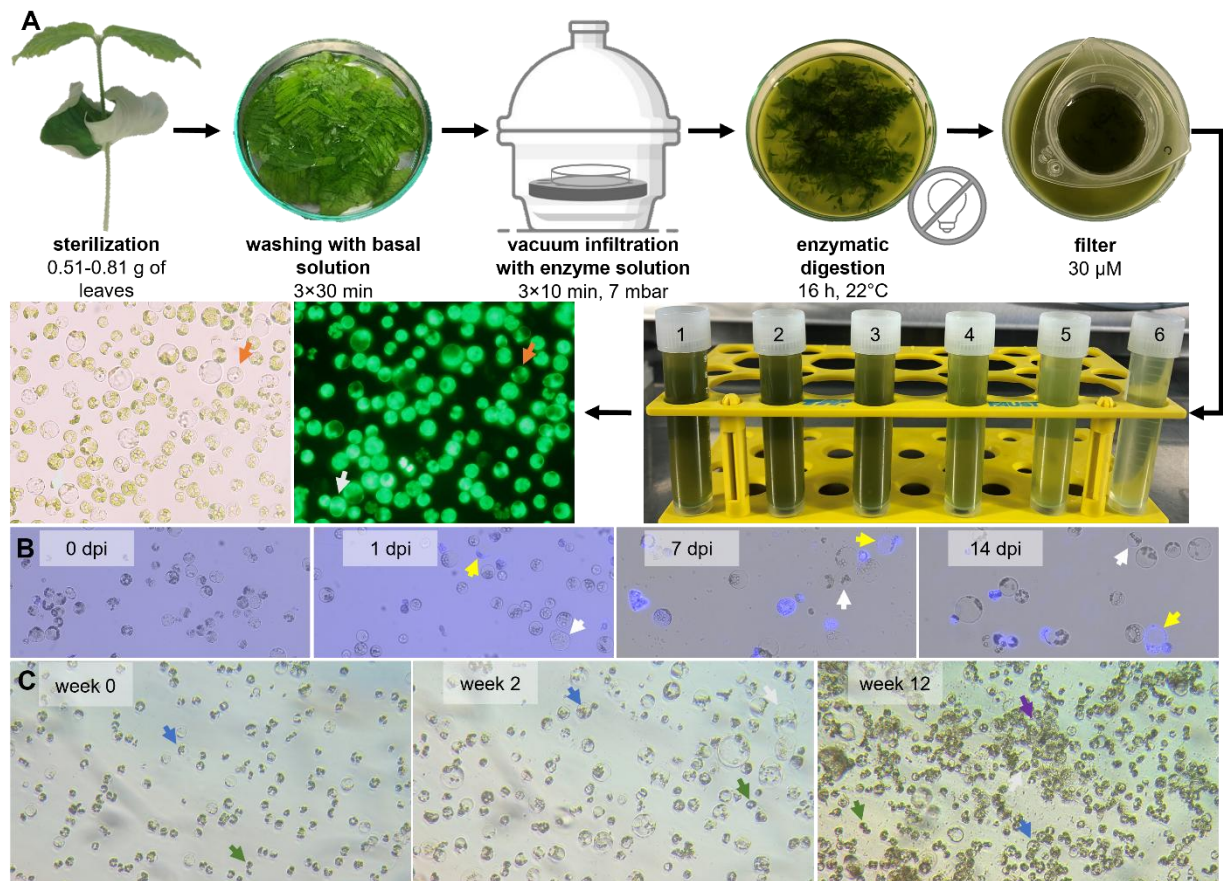
88 Results

89 Protoplast isolation and cultivation

90 We identified two discrete seasonal windows in which leaves were optimally suited for isolation: winter
91 to late spring (January–May) and autumn (September–November). Using the final protocol, an average
92 yield of 5.48×10^7 protoplasts g^{-1} FW (SD = 3.61×10^7) with a mean viability of 94.23% (SD = 3.49%)
93 was obtained, with maximum values reaching 1.46×10^8 protoplasts g^{-1} FW (Figure 1A; Table S1). A
94 subset of protoplasts exhibited strong viability fluorescence despite lacking chloroplasts, and rare
95 dividing protoplasts were observed. Calcofluor White staining confirmed complete cell wall removal
96 following isolation (Figure 1B). Cell wall regeneration initiated within 1 dpi, with uniform fluorescence
97 indicating full reformation by 7 dpi. Protoplasts subsequently proliferated, forming dense aggregates and
98 microcolonies by 12 weeks (Figure 1C). Contamination occurred in 5 of 126 wells (3.97%) and was
99 restricted to two of twelve isolations (Table S1). In initial tests, antibiotics did not reduce cell viability,

100 whereas addition of the fungicide natamycin caused extensive cell death across multiple replicates
101 (Figure S1).

102



103

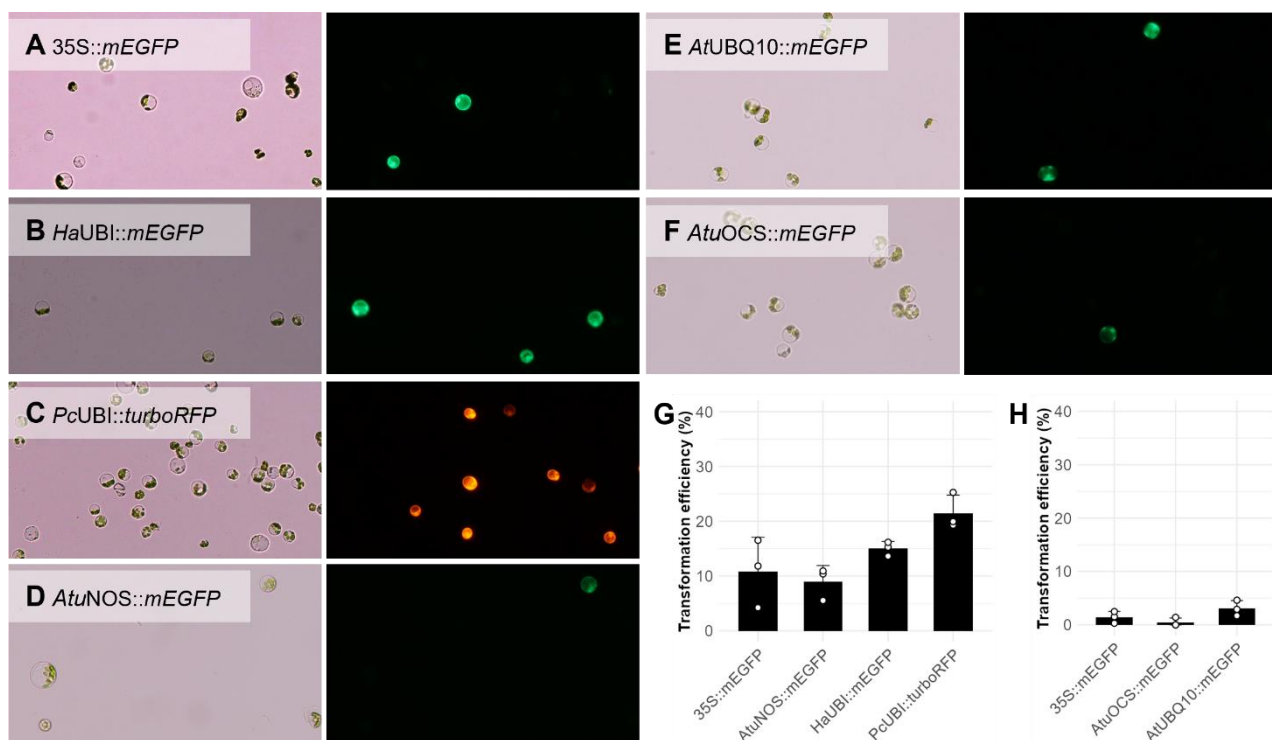
104 **Figure 1: Isolation and cultivation of protoplasts derived from beech seedling leaves.** (A)
105 Seedlings were grown *ex vitro*. The primary leaves were harvested, surface-sterilized, cut
106 into strips, and washed in basal solution. Subsequently, tissue was vacuum-infiltrated with
107 enzyme solution and digested overnight. The resulting suspension was filtered (tubes 1-
108 3), and residual tissue was washed three times with W5 solution to release additional
109 protoplasts (tubes 4-6). Filtrates were centrifuged, and the pooled pellets were
110 resuspended in W5 solution. The bright-field image (left) shows a heterogeneous
111 population consisting of chloroplast-containing and chloroplast-free protoplasts (orange
112 arrow). The FDA staining (right) confirmed the high viability of all observed protoplasts, as
113 indicated by strong green fluorescence. The white arrow highlights the rare observation of
114 a dividing protoplast detected within the isolate at day 0. (B) Calcofluor White staining
115 confirming remaining cell wall fragments by absence of fluorescence in freshly isolated
116 protoplasts (0 dpi). Within one day, the first signs of wall regeneration (yellow arrow) and
117 occasional cell divisions (white arrow) were observed. By 7 dpi, protoplasts displayed
118 uniform blue fluorescence, indicating full cell wall regeneration. Staining at 14 dpi

119 confirmed continued cell-wall presence. (C) Changes in protoplast morphology and growth
120 over time. Representative images at day 0, week 2, and week 12 in regeneration medium.
121 At day 0, all viable protoplasts are spherical single cells (blue arrow). By week 2,
122 protoplasts have begun to divide (white arrow). By week 12, multicellular clusters (purple
123 arrow) have formed. Over time, the presence of dead cells and cellular debris (green
124 arrow) increases.

125 Promoter-reporter validation

126 To establish a fundamental molecular toolbox for beech, a set of promoter-reporter constructs was
127 tested via transient expression in isolated protoplasts. This marks the first successful molecular
128 characterization of regulatory elements in this species. Successful transient expression of *mEGFP* or
129 *turboRFP* was achieved using six different constitutive promoters (Figure 2A–F). The promoters
130 exhibited a wide range of activity, quantified by transformation efficiency (the percentage of fluorescent
131 cells) across two independent transformation days (Figure 2G, H). The *PcUBI* promoter, driving
132 *turboRFP* expression, achieved the highest overall transformation efficiency observed in this study,
133 exceeding 20% (Figure 2G). All three tested *UBIQUITIN* promoters (*HaUBI*, *PcUBI*, and *AtUBQ10*)
134 generally exhibited higher activity than the *CaMV35S* promoter. Conversely, the *A. tumefaciens*-derived
135 promoters (*AtuNOS* and *AtuOCS*) showed lower transformation efficiencies compared to the *CaMV35S*
136 promoter on both transformation days. Both *mEGFP* and *turboRFP* reporter proteins were expressed
137 and fluorescently detectable, confirming their functionality in beech cells.

138



139

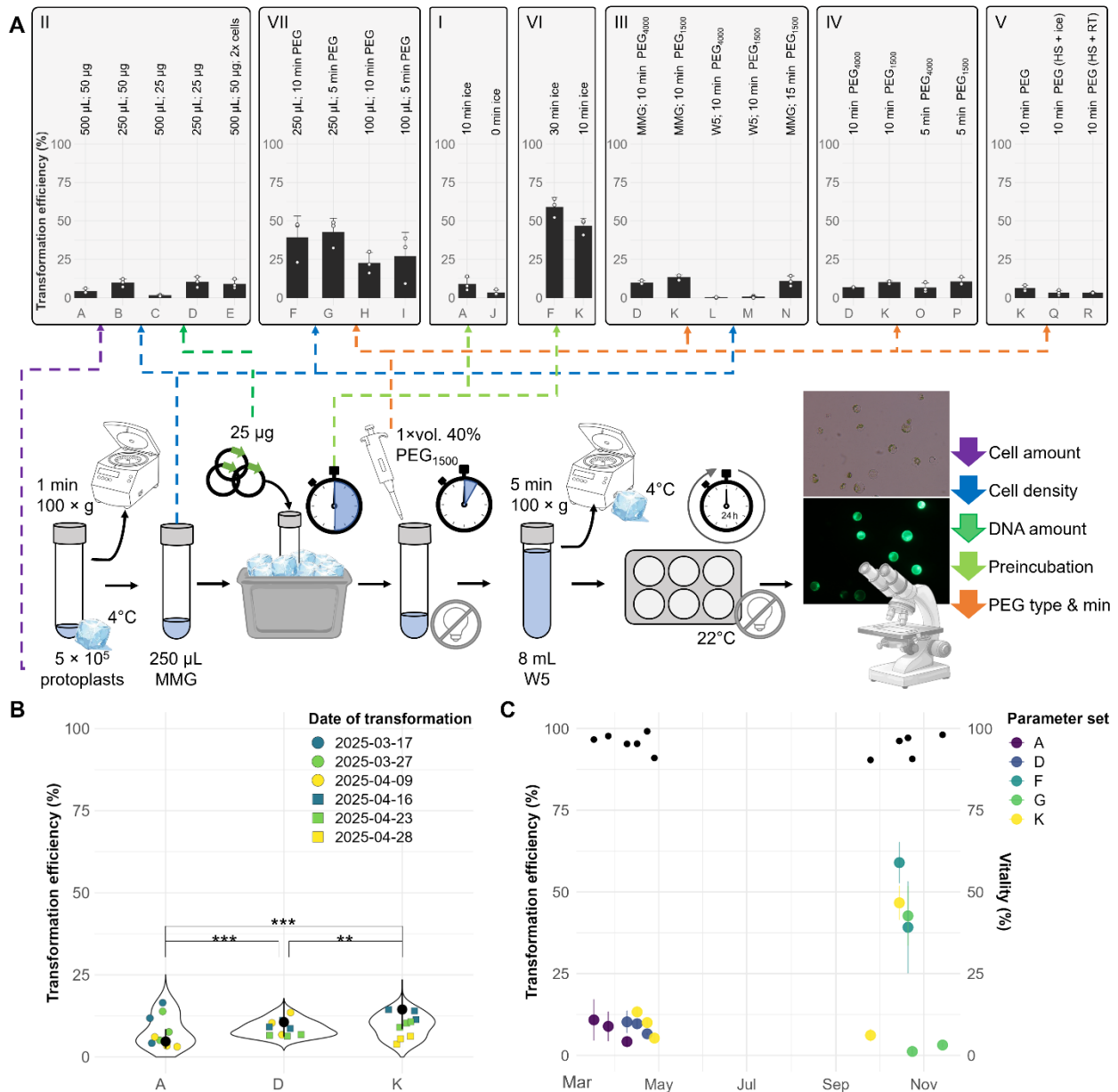
140 **Figure 2: Evaluation of reporter constructs in beech protoplasts.** (A–F) Bright-field (left) and
141 fluorescence (right) images of protoplasts after PEG-mediated transformation. (A–D)
142 Transformations using parameter set A (17/03/2025) with 35S::*mEGFP*, *HaUBI*::*mEGFP*,
143 *AtuNOS*::*mEGFP*, and *PcUBI*::*turboRFP*. (E, F) Transformations using parameter set G
144 (24/10/2025) with *AtUBQ10*::*mEGFP* and *AtuOCS*::*mEGFP*. No autofluorescence was
145 detected in untransformed protoplasts under identical imaging conditions (Figure S2). (G,
146 H) Transformation efficiencies of vectors transformed on (G) 17/03/2025 and (H)
147 24/10/2025. Dots represent technical replicates (n = 3), bars indicate mean transformation
148 efficiency, and error bars represent SD (Table S2).

149 PEG-mediated transformation and optimization

150 Seven independent transformation experiments (I–VII) were conducted to optimize the PEG-mediated
151 protocol sequentially, comparing parameter sets A–V (Figure 3; Table 1). Pre-incubation of protoplasts
152 with plasmid DNA on ice was found to be critical, with extending the pre-incubation to 30 min yielding
153 the highest efficiency (Figure 3A I, VI). Optimal cell density was determined to be 2×10^6 cells/mL using
154 a total amount of 5×10^5 protoplasts, which outperformed the lower density conditions. At this optimal
155 density, increasing the DNA (25 μ g vs 50 μ g) or protoplast amount (1×10^6) resulted in minor reductions
156 in efficiency (Figure 3A II). Further increasing the cell density by reducing the transfection buffer volume
157 decreased efficiency (Figure 3A VIII). MMG buffer resulted in higher transformation rates than W5
158 solution, irrespective of the PEG type used (Figure 3A III). Regarding the PEG treatment, PEG₁₅₀₀
159 slightly outperformed PEG₄₀₀₀ (Figure 3A III, IV). Within the PEG types, 5 min and 10 min incubations
160 yielded similar high efficiencies, while increasing the incubation time to 15 min led to reduced efficiencies
161 (Figure 3III). However, when the DNA pre-incubation on ice was extended to 30 min the 5 min PEG
162 incubation produced higher transformation efficiencies than the 10 min incubation (Figure 3VI).
163 Reducing the PEG concentration from 40% to 30% or 20% decreased transformation efficiencies under
164 all tested conditions (Table 1). Microscopic inspection confirmed that the decrease in efficiency was not
165 primarily due to morphological damage, as protoplasts largely retained their integrity even after extended
166 30% PEG treatment (Figure S3). Applying a 42°C heat shock for 1 min immediately after PEG addition
167 negatively impacted transformation efficiency, regardless of subsequent incubation conditions
168 (Figure 3A V).

169

First report of genetic transformation and CRISPR/Cas12a-mediated gene editing of European beech (*Fagus sylvatica* L.)
Zahn V, Sievers AJ, Kersten B, Fladung M, Bruegmann T



170

171 **Figure 3: Effect of experimental setup and transformation date on PEG-mediated gene**
 172 **delivery in beech protoplasts.** Protoplasts were transformed with the 35S::mEGFP
 173 reporter using parameter sets A–R (Table 2). Transformation efficiency (%) was defined
 174 as the proportion of GFP-positive cells relative to the total cell count (mean \pm SD of three
 175 technical replicates). See Data S1 and Table S3 for numerical values (A) Overview of
 176 optimization experiments (I–VII; chronological order). Dot and bar plots illustrate raw
 177 transformation efficiencies and corresponding means \pm SD for each parameter set.
 178 Parameter sets are grouped according to their position within the workflow and indicated
 179 by color-coded arrows, and key variables are summarized above each bar. The optimized
 180 workflow (parameter set G) is shown schematically. All experiments used
 181 5 \times 10⁵ protoplasts, except parameter set E (1 \times 10⁶; 2x cells). Protoplasts were
 182 centrifuged at 100 \times g for 1 min and resuspended in 500, 250, or 100 μ L of W5 or MMG.

183 Plasmid DNA (25 or 50 µg) was added and incubated on ice for 0, 10, or 30 min.
184 Transformation was induced by adding one volume of 40% PEG (PEG₄₀₀₀ or PEG₁₅₀₀) and
185 incubating for 5, 10, or 15 min in the dark. Alternatively, after PEG addition, heat shock
186 (HS) was performed at 42°C for 1 min followed by 9 min on ice or at RT. Reactions were
187 diluted to 8 mL with W5, centrifuged (5 min, 100 × g, 4°C), and incubated for 24 h at 22°C
188 in the dark. Transformation efficiency was quantified via fluorescence microscopy. (B)
189 Distribution and statistical comparison of transformation efficiencies for parameter sets A,
190 D and K across biological replicates. Violin plots display raw efficiencies from March and
191 April; points are color-coded by transformation date. Black dots represent Estimated
192 Marginal Means from the GLMM; error bars show 95% confidence intervals. Asterisks
193 indicate significant pairwise differences (*p < 0.05; **p < 0.01; ***p < 0.001). (C) Seasonal
194 variation in transformation efficiency and protoplast vitality. Mean efficiencies (± SD) of
195 parameter sets tested at least twice are shown in relation to the transformation date.
196 Protoplast vitality (%) after isolation (Evans Blue or FDA staining) is plotted as an
197 independent data layer (black dots; right-hand y-axis), enabling comparison between cell
198 viability and transformation performance.

199

200 **Table 1: Effect of varying PEG concentrations and incubation times on transformation**
201 **efficiency.** Transformation experiments were performed on two independent
202 transformation days (No.) with 5 × 10⁵ protoplasts in 250 (VI) or 100 µL (VII) MMG, and
203 25 µg plasmid DNA per reaction, using a PEG₁₅₀₀ solution. A pre-incubation on ice for 10
204 (VI) or 30 min (VII) was applied before PEG treatment. Transformation efficiency
205 represents mean ± SD of three technical replicates.

No.	Parameter set	PEG treatment	Transformation efficiency (mean ± SD) [%]
VI	K	10 min 40% PEG	46.69 ± 5.08
VI	S	20 min 20% PEG	7.42 ± 0.70
VII	H	10 min 40% PEG	22.54 ± 6.98
VII	I	5 min 40% PEG	26.90 ± 15.59
VII	T	40 min 30% PEG	12.80 ± 3.04
VII	U	40 min 20% PEG	6.91 ± 4.33
VII	V	20 min 30% PEG	13.11 ± 2.96

206

207 Transformation efficiencies of the same parameter set showed considerable variability across
208 independent experiments. In some cases, improved parameter sets yielded lower absolute efficiencies

209 than suboptimal conditions from earlier time points (Figure 3A I, II). Initial analysis of parameter sets A,
210 D, and K (n = 3 biological replicates) resulted in mean efficiencies of 7.98% ± 4.91%, 8.84% ± 2.49%,
211 and 9.53% ± 3.67%, respectively. A one-way ANOVA revealed no significant differences in efficiency
212 among the three groups (p = 0.847; Figure S4). However, in March and April, we observed a distinct
213 pattern where efficiency for the same parameter set consistently decreased over time (Figure 3B, C).
214 This temporal variation indicated a strong random effect of the transformation day on the outcome,
215 necessitating a different statistical approach. To account for this variation, a GLMM was applied,
216 including the transformation day as a random factor. A likelihood-ratio test revealed a significant overall
217 effect of the parameter sets on transformation efficiency ($\chi^2 = 29.67$, df = 2, p ≤ 0.001). Post-hoc analysis
218 using the EMMs with Tukey adjustment confirmed clear differences: parameter set K (14.48%, 95% CI:
219 8.48–23.64%) showed significantly higher efficiency than D (10.62%, 95% CI: 6.17–17.68%), which in
220 turn outperformed A (4.74%, 95% CI: 2.60–8.51%; Figure 3B). Model diagnostics indicated a generally
221 acceptable fit (p > 0.05), although the uniformity test (p = 0.088) suggested slight deviations from the
222 expected distribution, likely due to a lack of homogeneity for specific transformation days (23/04/25 and
223 28/04/25; Figure S5).

224 The first transformation in September yielded an efficiency comparable to the result obtained in April.
225 The peak transformation efficiency was reached in October, with up to 59.00 ± 6.19%, followed by a
226 sharp decline to 1.19 ± 0.87% (Figure 3C). The vitality of the protoplasts after isolation did not follow the
227 same trend as the transformation efficiencies over the course of the year. Altogether, sequential
228 optimization defined parameter set G as a suitable PEG-mediated transformation protocol for beech,
229 despite a significant temporal effect on transformation efficiency.

230 Identification of target gene *FsPDS*

231 Blasting the *Populus trichocarpa PDS* (*PtPDS*) gene sequence against the beech reference genome
232 resulted in the identification of a putative *FsPDS* gene (Bhaga_5.g3100). A subsequent BLAST search
233 using the putative *FsPDS* gene revealed the highest sequence similarity to *PDS* genes from *Fagaceae*
234 family members, particularly to *Quercus robur PDS* (*QrPDS*), which served as a reference for
235 subsequent structural and functional analyses (Table S4). The predicted *FsPDS* consists of 14 exons
236 (Figure 4A; Figure S6a). An additional *in silico* predicted exon introducing a premature stop codon was
237 excluded from the final gene model (Figure S6a). Exon 1 was added to the gene model by sequence
238 homology to the *Fagaceae* species and was validated by the identified N-terminal chloroplast transit
239 peptide (Figure S6c). The resulting gene structure includes the chloroplast translocation peptide and an
240 amino oxidase domain architecture, which was found to be consistent with the highly homologous
241 *QrPDS* protein and the initial query sequence, *PtPDS* (Figure S6b, c).

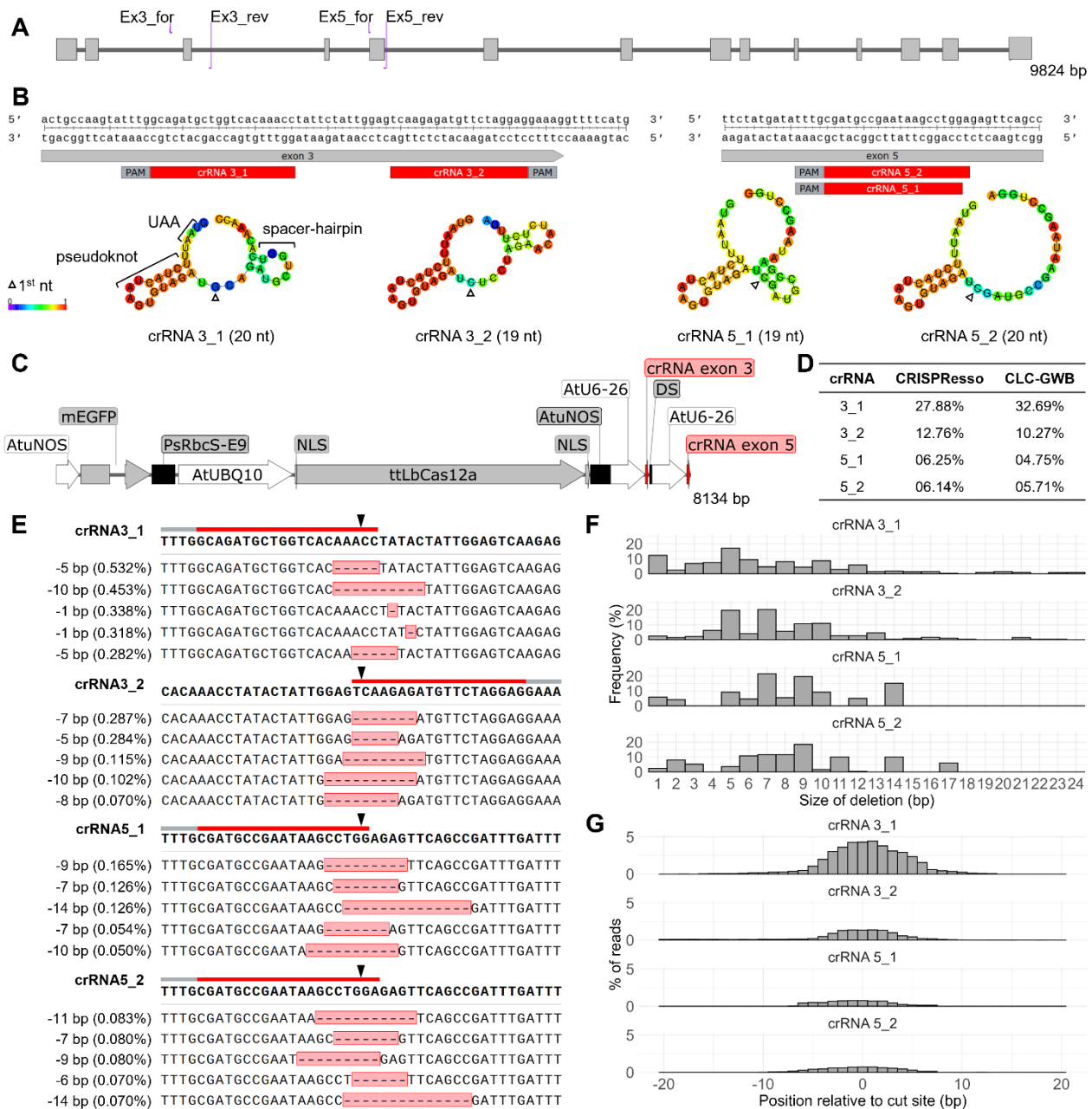
242 CRISPR/Cas-mediated editing of *FsPDS*

243 The modeled secondary structures of the gRNAs targeting *FsPDS* exons 3 and 5 predicted proper
244 pseudoknot folding and absence of strong spacer internal base-pairing (Figure 4B). CCTop predicted
245 medium editing efficiencies for both crRNA3_1 (0.66) and crRNA5_2 (0.62). To validate the functionality
246 of the CRISPR/Cas12a system in beech, two distinct vectors, *FsPDS*-KO1 and *FsPDS*-KO2 targeting
247 *FsPDS* with two gRNAs each (Figure 4C), were delivered into beech protoplasts using PEG-mediated
248 transformation (Table 3; Figure S7a, b). Successful delivery of the *ttLbCas12a* gene was confirmed via
249 PCR in all transformed samples.

250 Quantitative analyses of the amplicon sequencing yielded gene editing efficiencies in transformed cells
251 ranging from 4.75% to 32.69%, depending on crRNA and quantification method (Figure 4D; Table S5).
252 Top deletion patterns were unique for each crRNA used (Figure 4E). Deletion sizes ranged from 1 to
253 24 bp. Most frequent deletion sizes were 5 bp (crRNA3_1), 7 bp (crRNA3_2, crRNA5_1) and 9 bp
254 (crRNA5_2). Across all four crRNAs, deletion events were concentrated in the range of 5–10 bp
255 (Figure S8). Maximum deletion sizes were 24 bp (crRNA3_1), 21 bp (crRNA3_2), 14 bp (crRNA5_1)
256 and 17 bp (crRNA5_2) (Figure 4F). In the WT, only a minor number of 1- and 2-bp deletions were found
257 (Table S6). Subsequent deletion analysis revealed clear deletion peaks at the expected cleavage sites
258 for all four targets (Figure 4G), confirming target-specific *FsPDS* editing. No insertions were found at the
259 cut sites.

260

First report of genetic transformation and CRISPR/Cas12a-mediated gene editing of European beech (*Fagus sylvatica* L.)
Zahn V, Sievers AJ, Kersten B, Fladung M, Bruegmann T



261

262 **Figure 4: CRISPR/Cas12a-mediated editing of the *PHYTOENE DESATURASE* (*FsPDS*) gene in**
 263 **beech.** (A) The *FsPDS* gene consists of 14 exons. Positions of the PCR primers used for
 264 target amplification are indicated (Ex3_for, Ex3_rev; Ex5_for, Ex5_rev). (B) Target regions
 265 within exon 3 and 5 are shown in magnified views, with the crRNA spacers (red) and the
 266 PAM (grey). *In silico* predicted secondary (centroid) structures of the crRNAs are shown
 267 with color-coded base pairing probabilities. The first target-determining nucleotide for each
 268 crRNA spacer is indicated. Structural features associated with crRNA efficiency are
 269 exemplarily highlighted for crRNA 3_1. The crRNAs ending on 1 are part of the *FsPDS*-
 270 KO1 vector, and crRNAs ending on 2 were encoded by the *FsPDS*-KO2 vector. (C) Partial
 271 schematic map of the vectors (*FsPDS*-KO1 and *FsPDS*-KO2) used for protoplast
 272 transformation. Each vector contains four expression cassettes consisting either of a

273 coding sequence (grey) or a crRNA transcriptional unit (red), each flanked by a specific
274 promoter (white) and terminator (black): (1) monomeric enhanced green fluorescent
275 protein (mEGFP), (2) temperature-tolerant *LbCas12a* (ttLbCas12a) with two nuclear
276 localization signals (NLS), (3+4) crRNA targeting exon 3 and exon 5 of *FsPDS* separated
277 by a termination sequence (DS). (D) Editing efficiencies of individual crRNAs obtained
278 using CRISPResso 2.0 or CLC Genomics Workbench (CLC-GWB) in consideration of
279 transformation efficiencies. (E-G) CLC-GWB-based deletion analysis for each crRNA
280 targeting *FsPDS*. (E) Top 5 deletion patterns. PAM (grey bar), spacer sequences (red
281 bars), and cut sites (black triangles) are indicated above the WT reference sequence (first
282 row). The frequency of a specific deletion pattern (bp) in relation to read coverage is
283 indicated (%). (F) Distribution of deletion sizes, shown as the frequency (%) of each
284 deletion size within all deletions. (G) Distribution of deletions within ± 20 bp of the cut site,
285 expressed as a percentage of total reads.

286 **Table 1: Transformation efficiency of beech protoplasts using CRISPR/ttLbCas12a vectors.**
287 Efficiency [%] was quantified as the percentage of green fluorescent cells relative to the
288 total cell count. Mean efficiency is presented for each vector based on three independent
289 technical replicates (Rep I-III; n = 3).

Vector	Transformation efficiency [%]			Transformation efficiency (mean \pm SD) [%]
	Rep I	Rep II	Rep III	
FsPDS-KO1	11.20	17.29	10.28	12.92 \pm 3.81
FsPDS-KO2	8.43	6.53	14.34	9.79 \pm 4.05

290

291 Discussion

292 Protoplast isolation and cultivation

293 We present a reproducible protocol for the isolation of beech protoplasts with high yield, which achieves
294 excellent viability. This provides a robust foundation for functional studies in this woody species.

295 Seasonal and developmental factors strongly influenced isolation success. Highest yields were obtained
296 from soft primary leaves shortly after emergence, during late winter to early summer and in autumn.
297 Rapid leaf hardening outside these periods markedly reduced efficiency, even under constant growth
298 conditions. This pattern is consistent with seasonally programmed rhythms reported for beech seedling
299 development, as well as seasonal variation in protoplast yield in other species (García-Plazaola et al.,
300 2017; Keskitalo, 2001; Zahn et al., 2025), suggesting that comparable effects may occur in other
301 genotypes or plants. The negative effect of leaf hardening on isolation is consistent with earlier reports

302 for beech and other woody species (Ahuja, 1984; Choury et al., 2018; Han et al., 2023; Lang and
303 Kohlenbach, 1988). Aligning isolation with these periods enabled yields of up to
304 1.46×10^8 protoplasts g^{-1} FW with high viability. These values fall within the upper range reported for
305 woody species and extend material availability in beech beyond the narrow spring flush typically used,
306 while avoiding the labor-intensive and variable outcomes associated with forced bud break (Ahuja, 1984;
307 Kuzminsky et al., 2016; Lang and Kohlenbach, 1988; Yang et al., 2024). Observed variability across
308 replicates highlights the sensitivity of the procedure to leaf physiology and genotype, consistent with
309 prior reports in *Fagaceae* (Ahuja, 1984; Butt, 1985; Gülz et al., 1992; Yang et al., 2022).

310 Contamination control and antifungal sensitivity are critical. Mild surface sterilization combined with
311 antimicrobial agents maintained low contamination and high viability. However, when added to the
312 regeneration medium, natamycin caused rapid protoplast death, likely through non-specific interactions
313 with membrane sterols (Hsueh et al., 2007; te Welscher et al., 2008), emphasizing the need for careful
314 antifungal selection in wall-less plant cells.

315 The presence of chloroplast-free but viable protoplasts reflects inherent cellular heterogeneity, which is
316 known in leaf-derived protoplast populations (Han et al., 2023) and should be considered in downstream
317 experiments. Rapid cell wall regeneration and early proliferation indicate high physiological competence,
318 supporting the improved regeneration compared with earlier reports in beech (Ahuja, 1984; Reed and
319 Bargmann, 2021).

320 **Promoter-reporter validation**

321 The functionality of six constitutive promoters (*CaMV35S*, *AtuNOS*, *AtuOCS*, *AtUBQ10*, *HaUBI*, *PcUBI*)
322 was successfully confirmed via transient expression using mEGFP or turboRFP reporters in beech
323 protoplasts. The resulting trend in transformation efficiencies is likely attributed to two factors: inherent
324 differences in the transcriptional activity of the tested promoters and the superior performance of the
325 turboRFP reporter, specifically its rapid maturation and higher intrinsic brightness compared to mEGFP
326 (Merzlyak et al., 2007). Consistent with present data, the *UBIQUITIN* promoters generally drive higher
327 gene expression compared to *CaMV35S*, whereas the *AtuNOS* and *AtuOCS* promoters are significantly
328 weaker (Horstmann et al., 2004; Kishi-Kaboshi et al., 2019; Ni et al., 1995; Wolabu et al., 2020). Both
329 transcriptional activity and reporter properties influence the apparent brightness, thereby affecting the
330 detection rate of transformed cells. Although a rigorous quantitative ranking of their absolute strength
331 requires future plate-reader assays or flow cytometry, the confirmed functionality of these diverse
332 promoters establishes the foundational molecular toolbox necessary for future transgenic studies in
333 beech.

334 PEG-mediated transformation and optimization

335 We successfully optimized the PEG-mediated transient transformation protocol for beech, achieving a
336 peak efficiency of 59% (Figure 3) and establishing a reliable basis for transient expression assays.

337 Pre-incubation of DNA with protoplasts on ice for 30 min in Ca²⁺-containing MMG buffer was critical for
338 maximizing efficiency at the reduced PEG incubation time (5 min), likely by promoting transient DNA–
339 membrane interactions while protecting the plasmid from nucleases (Folling et al., 1998; Kinraide and
340 Wang, 2010).

341 Transfection conditions were critical: MMG buffer (15 mM CaCl₂) outperformed W5 (125 mM CaCl₂),
342 highlighting the importance of adequate cation concentration for DNA–membrane bridging and complex
343 stabilization (Kinraide and Wang, 2010; Masani et al., 2014; Yoo et al., 2007). Doubling cell density from
344 1 × 10⁶ cells/mL to 2 × 10⁶ cells/mL markedly increased transformation efficiency, likely due to closer
345 cell–DNA contact. Further increases in DNA (from 25 to 50 µg) or cell density (up to 1 × 10⁷ cells/mL)
346 did not improve efficiency, an effect also observed in woody plants, which may reflect saturation of
347 uptake sites or crowding at high cell density (Masani et al., 2014; Zhao et al., 2025).

348 Beech protoplasts are highly sensitive to osmotic and chemical stress. PEG₁₅₀₀ consistently yielded
349 higher transformation efficiencies than PEG₄₀₀₀, which may reflect lower cytotoxicity associated with
350 lower molecular weight PEG (Hong et al., 2023). Although rarely used in plant protocols, it appears
351 suitable for PEG-sensitive species (Bruegmann et al., 2019b). DNA uptake saturates within minutes,
352 making the 5-min PEG incubation critical. Longer exposure likely reduces efficiency due to stress. In
353 other species, optima can reach 30 min under the same PEG concentration (Bai et al., 2020),
354 highlighting the high PEG sensitivity of beech. High PEG concentrations (40%) were necessary to
355 achieve efficient DNA delivery (Table 1), whereas species with higher baseline efficiencies can suffice
356 with lower, less cytotoxic concentrations (20%) (Yang et al., 2022). Heat shock, sometimes applied in
357 other woody plants, proved detrimental in beech, likely exacerbating PEG-induced membrane stress
358 (Huo et al., 2017; Lei et al., 2024; Weigel, 1983; Ye et al., 2023; Zhou et al., 2024a).

359 Despite protocol optimization, transformation efficiency in beech remained consistently low (approx.
360 10 %) compared to model systems (e.g., *Populus* 80 %) or other non-model forest tree species (e.g.,
361 *Fraxinus excelsior* 67%, *Quercus ilex* 62%) (Lu et al., 2025; Pavese et al., 2024; Tan et al., 2013; Zhang
362 et al., 2016). High cell viability and effective cell wall removal confirmed that the low baseline was not
363 due to technical failure. Instead, a major limiting factor was marked temporal variability across biological
364 replicates, with efficiencies strongly correlated with the date of transformation. Temporal variation was
365 accounted for in statistics, but residual differences may reflect external factors such as water stress (Yoo
366 et al., 2007). These fluctuations suggest an underlying endogenous, circannual rhythm, consistent with
367 our observations in beech protoplast isolation and seedling responses to *in vitro* conditions (Zahn et al.,
368 2025). This rhythm likely influences the protoplasts' physiological response to transformation, affecting
369 PEG stress tolerance and DNA uptake. Consistent with this, a 5-min PEG incubation was essential even

370 under optimal conditions, as DNA uptake saturates rapidly and longer exposure reduces efficiency.
371 Species-specific recalcitrance and heterogeneous genotypes may also contribute to the low baseline
372 efficiency (Yang et al., 2022).

373 Although transformation efficiencies of approx. 50% are often considered desirable for downstream
374 applications (Yoo et al., 2007), achieving a baseline efficiency of around 10% represents an important
375 first milestone for beech, for which no protoplast transformation system has previously been established.
376 While transformation efficiency showed pronounced temporal variability, the present work provides a
377 reproducible and experimentally accessible framework for transient expression assays. Further
378 optimization should focus on improving temporal stability. Overall, this protocol lays a solid foundation
379 for functional studies and genome editing in beech and substantially expands the experimental toolbox
380 for this species.

381 **CRISPR/Cas-mediated editing of *FsPDS***

382 The successful detection of deletions at all four target sites demonstrates the functionality of the
383 *ttLbCas12a* system in beech protoplasts, a notable finding given the limited reports of Cas12a in woody
384 plants (Das et al., 2025; Jia et al., 2022). Editing efficiencies varied between crRNAs, reaching up to
385 32.7 % for crRNA3_1, similar to stable poplar transformations with (*ttLbCas12a*) (An et al., 2020; Das et
386 al., 2025). This is particularly noteworthy given that editing efficiencies in transient protoplast systems
387 are typically much lower than in stable lines (Gao et al., 2015; Zhang et al., 2023).

388 Observed differences in crRNA efficiency align with literature on crRNA sequence- and secondary
389 structure-dependent effects (Creutzburg et al., 2020; Kim et al., 2016; Li et al., 2023; Zhang et al., 2023).
390 Our design prioritized proper pseudoknot formation, yet modeling revealed variations in spacer hairpins
391 and base-pairing, likely influencing activity (Creutzburg et al., 2020). Minimal seed-region pairing
392 (crRNA3_1) was tolerated, whereas stronger pairing (crRNA5_1) may reduce cleavage efficiency
393 (Creutzburg et al., 2020; Zetsche et al., 2015). Other factors, such as UU motifs, spacer pairing position,
394 hairpin loop size, and modeling uncertainties (e.g., exclusion of the poly-U tail), further complicate the
395 prediction of crRNA efficiency (Creutzburg et al., 2020; Zhu and Liang, 2019). In addition, computational
396 tools such as CCTop were insufficient to reliably rank crRNAs. Together, these observations highlight
397 the necessity of empirical validation, particularly in perennial species where stable transformation is
398 time-consuming. Transient protoplast assays provide a rapid *in vivo* platform to assess crRNA efficacy
399 and identify highly active guides before stable transformation (Naim et al., 2020; Panda et al., 2024;
400 Sagarbarria et al., 2023).

401 Editing of *FsPDS* using *ttLbCas12a* resulted exclusively in deletions ranging from 1 to 24 bp, with
402 distinct, crRNA-dependent mutational patterns, consistent with observations in poplar and pummelo (An
403 et al., 2020; Das et al., 2025; Jia et al., 2022; Li et al., 2023; Zhang et al., 2023). Across the four crRNAs,
404 deletions predominantly clustered between 5–10 bp, in line with Cas12a editing in other plants
405 (Bernabé-Orts et al., 2019; Ma et al., 2024). 1-bp deletions, except for crRNA 5_1, might be considered

406 sequencing artifacts. Editing efficiencies estimated by CRISPResso and manual analyses were highly
407 similar, preserving the relative ranking of crRNAs, though manual analysis captured complex or low-
408 frequency deletion patterns more effectively.

409 Overall, these results demonstrate that *ttLbCas12a* induces a characteristic, crRNA-dependent deletion
410 spectrum in beech, closely matching outcomes in other woody and herbaceous species. Our findings
411 confirm the system's suitability for targeted genome editing and emphasize the importance of empirical
412 crRNA validation for efficient editing in perennial plants.

413 **Conclusions**

414 The optimization of protoplast isolation and transient transformation for beech provides a robust, high-
415 yield system, achieving up to 1.46×10^8 protoplasts g^{-1} FW and a peak transient efficiency of 59%. This
416 was accomplished by addressing key biological constraints, including the need to align preparations
417 with the endogenous circannual rhythm and by developing protocols that accommodate the pronounced
418 PEG sensitivity of beech protoplasts. We further established a foundational, MoClo-compatible
419 molecular toolbox using functional promoters and demonstrated the first successful application of
420 *ttLbCas12a*-mediated genome editing in beech, reaching editing efficiencies of up to 32.69%. While the
421 inherently low and temporally variable transformation efficiencies require further optimization, the
422 protoplast platform presented here provides a powerful and rapid *in vivo* validation system for targeted
423 genome editing in woody species and establishes a strong foundation for future functional genomics
424 and genome editing studies in beech.

425 **Experimental procedures**

426 **Plant material**

427 Beech nuts were collected in autumn 2024 in the arboretum of the Thünen Institute, Grosshansdorf,
428 Germany. The seeds were stored cool and dark until germination. Germination was initiated in darkness
429 at 4°C in moist clay granulate until the radicles emerged (January to May and September to November
430 2025). Seedling development was carried out at 22°C under a 16-hour photoperiod ($70 \mu\text{mol m}^{-2} \text{s}^{-1}$
431 photosynthetic photon flux density) in clay granulate in a climate chamber. The expansion of the primary
432 leaves took approx. three weeks.

433 **Protoplast isolation**

434 Protoplast isolation was performed using a protocol adapted from Bruegmann et al. (2019b). Unless
435 stated otherwise, all experiments were performed using the finalized protocol. Primary leaves were
436 harvested 24–48 h after unfolding (Figure 1A). Leaf samples (0.51–0.81 g) were washed in 1% alkaline
437 detergent solution and surface-sterilized with 0.12% NaClO containing 0.1% Tween-20 for 10 min,

438 followed by rinsing with sterile water. Cleaned leaves were cut into approx. 3 mm wide strips and washed
439 3 times for 30 min in basal solution (10 mM CaCl₂, 0.2 mM KH₂PO₄, 1 mM KNO₃, 1 mM MgSO₄·7H₂O,
440 5 mM MES, 1% PVP-10; adjusted to 600 mOsmol/kg with mannitol, pH 5.6).

441 The enzyme solution (2% (w/v) cellulase, 1% (w/v) macerozyme, 10 mM CaCl₂, 1 mM KH₂PO₄, 1 mM
442 MgSO₄, 20 mM MES, 2% (w/v) PVP-40, and 0.25% (w/v) BSA; adjusted to 600 mOsmol/kg with
443 mannitol, pH 5.6) was heated to 40°C for 10 min, and supplemented with antibiotics (500 mg/L
444 cefotaxime, 50 mg/L gentamicin, 50 mg/L streptomycin) and fungicide (10 mg/L natamycin). 25 mL of
445 enzyme solution was added to the leaf strips before vacuum infiltration 3 times for 10 min at 7 mbar.
446 Enzymatic digestion was carried out at 22°C in the dark for 16 h (4 rpm on an orbital shaker). The
447 resulting suspension was filtered through a 30 µm nylon mesh (Lang and Kohlenbach, 1988). The
448 remaining tissue was washed 3 times with 10 mL W5 solution with repeated filtering. Protoplasts were
449 collected by centrifugation at 50 × g for 6 min, and the pooled protoplasts were resuspended in W5
450 solution. Protoplast yield was quantified using a hemocytometer. In preliminary experiments, protoplast
451 viability was assessed using Evans Blue (400 mg/L in 0.5 M mannitol), mixed 1:1 (v/v) with the protoplast
452 suspension, whereas fluorescein diacetate (FDA) staining was used for all subsequent experiments
453 (Bruegmann et al., 2019b).

454 **Protoplast culture**

455 Protoplasts were cultured at a 2 × 10⁵ cells/mL density in regeneration medium (Murashige and Skoog
456 medium including vitamins, 0.01 µM thidiazuron (TDZ), 14 µM 2,4-dichlorophenoxyacetic acid (2,4-D);
457 adjusted to 600 mOsmol/kg with glucose/mannitol (2:1), pH 5.6; modified from Nietsch et al. (2017)) in
458 6-well plates at 22°C in the dark to assess sterility of the isolation procedure and protoplast development,
459 unless all protoplasts were used for transformation. To evaluate the effect of antimicrobial agents during
460 protoplast culture in initial experiments, the antibiotics only and the antibiotics in combination with the
461 fungicide in the concentrations mentioned above were added to the regeneration medium. The medium
462 was exchanged every 6 weeks. To monitor cell wall regeneration, 5 × 10⁵ protoplasts were suspended
463 in 1 mL of regeneration medium and cultivated in a 10 mL round-bottom centrifuge tube at 22°C in the
464 dark until cell wall staining.

465 **Cell wall staining**

466 Staining of protoplasts, either to assess the presence of residual cell wall fragments after isolation or to
467 visualize cell wall regeneration over time in regeneration medium, was performed using Calcofluor
468 White. For staining, Calcofluor White (1 g/L; Sigma-Aldrich) was added to protoplast suspensions in W5
469 solution (after isolation) or in regeneration medium (after cultivation) at a final dilution of 1:10 (v/v)
470 (Neubauer et al., 2022). After 2 min incubation at RT in the dark, the protoplasts were centrifuged at
471 60 × g for 3 min. The supernatant was discarded. The protoplasts were washed with W5 solution and
472 finally resuspended in 50 µL W5. 20 µL of protoplasts were used for fluorescence microscopy.

473 Cloning of promoter–reporter constructs

474 Expression vectors for promoter and reporter gene analysis in beech were assembled using the Modular
475 Cloning (MoClo) system (Marillonnet and Grütner, 2020). Modules from the MoClo Plant Parts Kit were
476 complemented with additional elements (Table S7). To ensure compatibility with MoClo, internal *Bsa*I
477 and *Bp*I recognition sites within the additional elements were removed by PCR-based site-directed
478 mutagenesis (Table S8). All primers for cloning are listed in the supplements (Table S9).

479 Level-1 (L1) expression vectors were generated, including constructs expressing the monomeric
480 Enhanced Green Fluorescent Protein (mEGFP) under the control of the CaMV35S promoter with the
481 TMV- Ω 5'UTR (35S::*mEGFP*), the *Arabidopsis thaliana* *UBIQUITIN10* promoter including 5'UTR and
482 first intron (*AtUBQ10::mEGFP*), the *Helianthus annuus* *POLYUBIQUITIN HaUBI* promoter
483 (*HaUBI::mEGFP*), the *Agrobacterium tumefaciens* *NOPALINE SYNTHASE* promoter
484 (*AtuNOS::mEGFP*) and the *A. tumefaciens* *OCTOPINE SYNTHASE* promoter (*AtuOCS::mEGFP*).
485 Transcription was stopped by *A. thaliana* HEAT SHOCK PROTEIN 18.2 (*AtHSP18.2*) terminator.
486 Additionally, a turboRFP construct with the *Petroselinum crispum* *UBIQUITIN* promoter and *Pisum*
487 *sativum* *pea3A* terminator was generated (*PcUBI::turboRFP*). All vector sequences (.dna files) are
488 available in Data S2.

489 Validation of genome editing target

490 Using BLAST analysis based on the *PDS* gene sequence from *PtPDS* (Potri.014G148700), the target
491 gene was identified in beech using the reference genome from (Mishra et al., 2021). The target regions
492 of *FsPDS* were additionally verified in northern German beech individuals by PCR amplification and
493 subsequent Sanger sequencing (Table S9). The exon-intron structure was predicted *in silico* using
494 FGENESH (Softberry Inc., <http://www.softberry.com>), employing *P. trichocarpa* as a reference.
495 Predicted exons, the annotated *PtPDS* gene, and mRNA sequences of tree species from the *Fagaceae*
496 family were aligned to the *FsPDS* sequence to support exon identification. Species were selected based
497 on the highest homology using the NCBI BLAST search. Sequence alignments were made using
498 SnapGene software (Dotmatics, Boston, MA, USA). Protein domains were annotated for the predicted
499 *FsPDS* protein in SMART (Letunic et al., 2021), and signal peptides were screened using TargetP-2.0
500 (Almagro Armenteros et al., 2019). The resulting annotations were compared to protein sequences
501 derived from *PtPDS* and *QrPDS* (belonging to the *Fagaceae* family) to support the structural and
502 functional analysis.

503 gRNA and editing vector design

504 CRISPR/Cas12a target sites were identified by scanning exon regions of the *FsPDS* gene for the
505 canonical TTTV PAM. Spacer sequences (19–24 nt) complementary to the target DNA were selected.
506 A non-canonical AsCas12a-derived direct repeat was used (Zetsche et al., 2015), which is compatible
507 with *LbCas12a* (Nguyen et al., 2024). A 5' G was added to support U6 promoter–driven transcription

508 (Shan et al., 2013), and transcription termination was achieved using a 7×T tail (Verosloff et al., 2021).
509 Secondary structures were predicted using RNAfold (Lorenz et al., 2011) with RNA parameters from
510 (Andronescu et al., 2007) at 22°C. Candidate crRNAs were prioritized based on stable pseudoknot
511 formation in the direct repeat, unpaired UAA motifs, minimal spacer self-complementarity, GC content
512 between 30–70%, and absence of homopolymeric triplets (Creutzburg et al., 2020; Zhu and Liang,
513 2019). Two crRNAs each targeting Exon 3 and Exon 5 were selected (5' – 3'): crRNA3_1
514 (gcagaugcuggucacaaacc), crRNA3_2 (ucaagagauguucuaggag), crRNA5_1 (cgaugccgaaauagccugg),
515 and crRNA5_2 (cgaugccgaaauagccugga). Predicted on- and off-target activities were assessed *in silico*
516 using CCTOP (Stemmer et al., 2015). The editing vectors FsPDS-KO1 and FsPDS-KO2 were obtained
517 from DNA Cloning Service (Hamburg, Germany). Each vector contained an AtU6-26::crRNA expression units targeting *FsPDS*. Fully
518 annotated vector sequences (.dna files) are provided in Data S2. The weak NOS promoter was used to
519 drive *mEGFP* expression, allowing prolonged incubation without detrimental cytotoxicity, while AtU6-26
520 and AtUBQ10 promoters were selected to ensure robust crRNA and *ttLbCas12a* expression,
521 respectively, based on their reported efficacy in plant systems (Bruegmann et al., 2019a; Castel et al.,
522 2019; Horstmann et al., 2004; Li et al., 2007; Lu et al., 2025; Walawage et al., 2019; Wolabu et al.,
523 2020).

525 PEG-mediated transformation

526 Protoplast transformation was performed using a PEG-mediated protocol adapted from (Bruegmann et
527 al., 2019b). Freshly isolated protoplasts stored in W5 solution at 4°C were used. Key transformation
528 parameters were optimized using a 35S::mEGFP reporter construct (Table 2). For the final protocol
529 (parameter set G), 5×10^5 protoplasts were resuspended in 250 μ L MMG solution and incubated with
530 25 μ L plasmid DNA ($1 \mu\text{g } \mu\text{L}^{-1}$; PureYield Plasmid Miniprep System; Promega, Madison, WI, USA) on
531 ice for 30 min. PEG₁₅₀₀ (40%) was added at a 1:1 ratio, followed by incubation for 5 min in the dark. The
532 reaction was terminated by stepwise addition of 8 mL W5 solution and centrifugation at $100 \times g$ for 5 min
533 at 4°C. Protoplasts were resuspended in regeneration medium at $2 \times 10^5 \text{ mL}^{-1}$ and incubated in 6-well
534 plates at 22°C in the dark for 24 or 48 h (CRISPR/Cas vectors only).

535 Reporter constructs were transformed using parameter sets A and G in two independent experiments;
536 CRISPR/Cas vectors used parameter set K (50 μg DNA). Three technical replicates were performed per
537 parameter set or vector. Transformation efficiency was quantified by fluorescence microscopy as the
538 percentage of mEGFP-positive cells. Values are reported as mean \pm SD. For microscopy, protoplasts
539 were released from plates by incubation with enzyme solution for 2 h at room temperature, pooled,
540 centrifuged ($100 \times g$, 5 min, 4°C), and resuspended for observation.

541

542 **Table 2: Parameter sets tested during the optimization of the PEG-mediated transformation**
 543 **protocol.** In all transformations, 5×10^5 protoplasts were used, except for E, where
 544 1×10^6 protoplasts were used. For the heat shock (HS), cells were incubated for 1 min
 545 at 42°C and 9 min at room temperature (RT) or on ice. Each parameter set was used on
 546 at least one transformation day during the optimization (No.).

Name	Transfection buffer	DNA [µg]	Ice [min]	PEG type	PEG [%]	PEG [min]	No.
A	500 µL MMG	50	10	4000	40	10	I, II
B	250 µL MMG	50	10	4000	40	10	II
C	500 µL MMG	25	10	4000	40	10	II
D	250 µL MMG	25	10	4000	40	10	II, III, IV
E	500 µL MMG	50	10	4000	40	10	II
F	250 µL MMG	25	30	1500	40	10	VI, VII
G	250 µL MMG	25	30	1500	40	5	VII
H	100 µL MMG	25	30	1500	40	10	VII
I	100 µL MMG	25	30	1500	40	5	VII
L	250 µL W5	25	10	4000	40	10	III
K	250 µL MMG	25	10	1500	40	10	III, IV, V, VI
M	250 µL W5	25	10	1500	40	10	III
N	250 µL MMG	25	10	1500	40	15	III
O	250 µL MMG	25	10	4000	40	5	IV
P	250 µL MMG	25	10	1500	40	5	IV
J	500 µL MMG	50	0	4000	40	10	I
Q	250 µL MMG	25	10	1500	40	10 (HS + ice)	V
R	250 µL MMG	25	10	1500	40	10 (HS + RT)	V
S	250 µL MMG	25	10	1500	20	20	VI
T	250 µL MMG	25	30	1500	30	40	VII
U	250 µL MMG	25	30	1500	20	40	VII
V	250 µL MMG	25	30	1500	30	20	VII

547

548 **Microscopy**

549 Protoplast counting, viability assessment by Evans Blue, and morphological checks were performed
 550 using an inverted light microscope. Fluorescence microscopy of FDA- and Calcofluor White-stained
 551 protoplasts, as well as of transformed cells, was conducted on an Axioscope 3 fluorescence microscope
 552 (Carl Zeiss Microscopy, Jena, Germany). Filter sets were as follows: mEGFP and FDA 469/38 nm (Ex)
 553 / 520–550 nm (Em); turboRFP 555/30 nm (Ex) / 600–650 nm (Em); Calcofluor White 385/30 nm (Ex) /
 554 445/50 nm (Em). ISO settings for transformed protoplasts were calibrated against PEG-treated wildtype

555 (WT) protoplasts to confirm absence of autofluorescence. Image analysis and cell counting were
556 performed using Fiji (Schindelin et al., 2012).

557 **Detection of genome editing events**

558 Genomic DNA was extracted from protoplasts transformed with CRISPR/Cas vectors FsPDS-KO1 or
559 FsPDS-KO2 (Bruegmann et al., 2022). The presence of *ttLbCas12a* was verified by standard PCR.
560 Target regions within *FsPDS* Exons 3 (Ex3; 415 bp) and 5 (Ex5; 175 bp) were amplified by PCR with
561 proof-reading active DNA Polymerase. PCR primer sequences are listed in Table S9. The amplified
562 target regions of the transformations with the highest transformation efficiency as well as the WT control,
563 were purified with the QIAquick PCR Purification Kit (QIAGEN, Hilden, Germany) and submitted to
564 GENEWIZ (Leipzig, Germany) for paired-end Illumina sequencing (2 × 250 bp). The fastq files from the
565 amplicon sequencing are available in the European Nucleotide Archive (ENA; Accession No.
566 PRJEB107651). The raw FastQ files were used for downstream indel analysis with the cutting side set
567 after the 18th nucleotide of the spacer sequence. For CRISPResso 2.0, the quantification window was
568 set at 10 bp, and substitutions were ignored (Clement et al., 2019). For further analysis of indels due to
569 insufficient results from CRISPResso, Illumina amplicon sequencing reads from six datasets (FsPDS-
570 KO1_Ex3/Ex5, FsPDS-KO2_Ex3/Ex5 and WT_Ex3/Ex5) were quality-trimmed and mapped to the
571 edited exon 3 or exon 5 reference sequences (Table S10) using CLC Genomics Workbench (QIAGEN,
572 Aarhus, Denmark). Variants, including rare variants, were detected, and indels overlapping the target
573 region (cut site ± 10 bp) were selected. The modification rate (%) was calculated as the number of
574 deletion-supporting reads divided by the mean coverage at the target site. Position-specific deletion
575 frequencies were determined by summing all deletions spanning each nucleotide position. Reads with
576 representative deletion patterns were selected based on BLAST analysis of sequences flanking the cut
577 site (± 20 bp) versus trimmed reads. Detailed trimming, mapping, variant calling, and BLAST parameters
578 are provided in Method S1. Editing rates were calculated by correcting the modification rates observed
579 in the target region, including the cut site for background changes in the WT control, and normalizing to
580 the transformation efficiency.

581 **Statistics and data visualization**

582 Statistical analyses and data visualizations were performed in RStudio v2024.12.0.467. Significance
583 was defined as $p \leq 0.05$. Parameter optimization results (n = 3 technical replicates) are reported as
584 mean ± SD. Transformation efficiency data (n = 3 biological replicates) were analyzed using one-way
585 ANOVA and generalized linear mixed models (GLMMs) to account for nested structure and binomial
586 count data. Model assumptions and diagnostics were assessed, and post hoc comparisons were
587 performed using estimated marginal means (Tukey method). Details on statistical analyses are
588 described in Method S2 and Data S3. For graphics with low percentage values, y-axis ranges were
589 adjusted to improve visual resolution.

590 **Authors' Contributions**

591 Study conception and design – V.Z., M.F., T.B.; methodology implementation – V.Z., A.-J.S., T.B.;
592 experiment execution – V.Z., A.-J.S.; data collection – V.Z.; data analysis/interpretation – V.Z., B.K.,
593 T.B.; manuscript writing/revision – V.Z., B.K., M.F., T.B.; funding acquisition – M.F., T.B.

594 **Acknowledgments**

595 We like to thank Susanne Jelkmann for her excellent laboratory assistance, Ina Martini for fluorescence
596 assays, and Friderieke Schwarzer for a BLAST search in the beech database genome. The work was
597 supported by the German Federal Ministry for Agriculture, Food, and Regional Identity (BMLEH) via the
598 Fachagentur Nachwachsende Rohstoffe within the project TreeEdit (grant 2219NR359). Open Access
599 funding enabled and organized by Project DEAL. This article is based upon work from COST Action
600 CA21157 “European Network for Innovative Woody Plant Cloning”, supported by COST (European
601 Cooperation in Science and Technology), www.cost.eu.

602 **Conflict of Interest**

603 The authors declare no conflict of interests.

604 **Data Availability**

605 Plasmids generated and used in this study are available from the corresponding author upon reasonable
606 request. Amplicon sequencing data have been deposited in ENA under accession number
607 PRJEB107651.

608 **Supplementary Data**

609 Method S1: Detection of genome editing events

610 Method S2: Statistics and data visualization

611 Figure S1: Beech protoplast viability after 5 (a-c) and 9 days (d-f) in different media

612 Figure S2: Negative control of protoplast transfection for promoter-reporter validation

613 Figure S3: Protoplast morphology and mEGFP expression of *F. sylvatica* protoplasts 24 h post-
614 transformation using PEG₁₅₀₀

615 Figure S4: QQ-plot of ANOVA residuals for protoplast transformation efficiencies (parameters A, D,
616 and F)

617 Figure S5: Diagnostic plots of GLMM for comparison of transformation parameters over time

- 618 Figure S6: Annotation of *F. sylvatica* *PHYTOENE DESATURASE* (*FsPDS*)
- 619 Figure S7: *F. sylvatica* protoplasts after transformation with the CRISPR/Cas12a vectors
- 620 Figure S8: Cumulative distribution of deletion sizes induced by *ttLbCas12a* across four crRNAs
621 targeting *FsPDS* in *F. sylvatica* protoplasts
- 622 Table S1: Protoplast isolation from *F. sylvatica* seedling leaves
- 623 Table S2: Transformation efficiencies of different promoter reporter constructs (vector) used for
624 *F. sylvatica* protoplast transformation
- 625 Table S3: Transformation efficiencies of different parameter sets used for *F. sylvatica* protoplast
626 transformation
- 627 Table S4: Highest ranked results of BLAST search of *FsPDS* gene against the NCBI database
- 628 Table S5: Quantification of WT-normalized modification rates and transformation-normalized editing
629 efficiencies for *FsPDS*-targeting crRNAs based on deletion frequencies (± 10 bp around the predicted
630 cut site) using CLC-GWB
- 631 Table S6: Deletions detected within ± 10 bp of the cut site for *FsPDS*-targeting crRNAs in the wildtype
632 control
- 633 Table S7: Level-0 (L0) modules used for cloning of L1 promoter-reporter constructs.
- 634 Table S8: Modifications of Level-0 modules for MoClo compatibility
- 635 Table S9: Primers used in this study
- 636 Table S10: Edited reference sequences of *FsPDS* exons 3 and 5 used for alignment of amplicon
637 sequencing data
- 638 Data S1: Raw data transformation optimization
- 639 Data S2: Vector and target sequences
- 640 Data S3: Statistical data

641 **References**

- 642 Ahuja, M. R. (1984) Short note: Isolation and culture of mesophyll protoplasts from mature beech
643 trees. *Silvae Genetica* **33**, 37–39.
- 644 Almagro Armenteros, J. J., Salvatore, M., Emanuelsson, O., Winther, O., Heijne, G. von, Elofsson, A.
645 and Nielsen, H. (2019) Detecting sequence signals in targeting peptides using deep learning. *Life*
646 *science alliance* **2**.
- 647 An, Y., Geng, Y., Yao, J., Fu, C., Lu, M., Wang, C. and Du, J. (2020) Efficient Genome Editing in
648 *Populus* Using CRISPR/Cas12a. *Frontiers in plant science* **11**, 593938.

- 649 Andronescu, M., Condon, A., Hoos, H. H., Mathews, D. H. and Murphy, K. P. (2007) Efficient
650 parameter estimation for RNA secondary structure prediction. *Bioinformatics (Oxford, England)* **23**,
651 i19-28.
- 652 Bai, L., Cheng, Y., She, J., He, Z., Liu, H., Zhang, G., Cao, R. and Chen, Y. (2020) Development of an
653 efficient protoplast isolation and transfection system for castor bean (*Ricinus communis* L.). *Plant*
654 *Cell Tiss Organ Cult* **143**, 457–464.
- 655 Baumbach, L., Niamir, A., Hickler, T. and Yousefpour, R. (2019) Regional adaptation of European
656 beech (*Fagus sylvatica*) to drought in Central European conditions considering environmental
657 suitability and economic implications. *Reg Environ Change* **19**, 1159–1174.
- 658 Bernabé-Orts, J. M., Casas-Rodrigo, I., Minguet, E. G., Landolfi, V., Garcia-Carpintero, V., Gianoglio,
659 S., Vázquez-Vilar, M., Granell, A. and Orzaez, D. (2019) Assessment of Cas12a-mediated gene
660 editing efficiency in plants. *Plant biotechnology journal* **17**, 1971–1984.
- 661 BMLEH [Bundesministerium für Landwirtschaft, Ernährung und Heimat] (2025). *Ergebnisse der*
662 *Waldzustandserhebung 2024*. Bonn.
- 663 Borthakur, D., Busov, V., Cao, X. H., Du, Q., Gailing, O., Isik, F., Ko, J.-H., Li, C., Li, Q., Niu, S., Qu,
664 G., Vu, T. H. G., Wang, X.-R., Wei, Z., Zhang, L. and Wei, H. (2022) Current status and trends in
665 forest genomics. *Forestry research* **2**, 11.
- 666 Bruegmann, T., Deecke, K. and Fladung, M. (2019a) Evaluating the Efficiency of gRNAs in
667 CRISPR/Cas9 Mediated Genome Editing in Poplars. *International journal of molecular sciences*
668 **20**.
- 669 Bruegmann, T., Fladung, M. and Schroeder, H. (2022) Flexible DNA isolation procedure for different
670 tree species as a convenient lab routine. *Silvae Genetica* **71**, 20–30.
- 671 Bruegmann, T., Polak, O., Deecke, K., Nietsch, J. and Fladung, M. (2019b) Poplar Transformation.
672 *Methods in molecular biology (Clifton, N.J.)* **1864**, 165–177.
- 673 Bussotti, F., Papitto, G., Di Martino, D., Cocciufa, C., Cindolo, C., Cenni, E., Bettini, D., Iacopetti, G.,
674 Ghelardini, L., Moricca, S., Panzavolta, T., Bracalini, M. and Pollastrini, M. (2024) Extreme climatic
675 events, biotic interactions and species-specific responses drive tree crown defoliation and mortality
676 in Italian forests. *iForest* **17**, 300–308.
- 677 Butt, A. D. (1985) A general method for the high-yield isolation of mesophyll protoplasts from
678 deciduous tree species. *Plant Science* **42**, 55–59.
- 679 Cao, H. X., Vu, G. T. H. and Gailing, O. (2022) From Genome Sequencing to CRISPR-Based Genome
680 Editing for Climate-Resilient Forest Trees. *International journal of molecular sciences* **23**.
- 681 Castel, B., Tomlinson, L., Locci, F., Yang, Y. and Jones, J. D. G. (2019) Optimization of T-DNA
682 architecture for Cas9-mediated mutagenesis in Arabidopsis. *PloS one* **14**, e0204778.
- 683 Chalupa, V. (1979) In vitro propagation of some broad-leaved forest trees. *Commun Inst For Āechosl*
684 **11**, 159–170.

- 685 Chen, X., Zhang, R., Yan, J., Jia, X., Liang, R., Sun, F., Li, L., Ma, M., Zhan, Y. and Zeng, F. (2025)
686 *Betula platyphylla* glucosyltransferase *BpGT14;6* is essential for cell wall development and stress
687 response. *Horticultural Plant Journal* **11**, 2267–2280.
- 688 Choury, Z., Meschini, R., Dell'Orso, A., Fardusi, M. J., Mugnozza, G. S. and Kuzminsky, E. (2018)
689 Optimized conditions for the isolation of mesophyll protoplasts along the growing season from
690 *Arbutus unedo* and their use in single cell gel electrophoresis. *Plant Cell Tiss Organ Cult* **132**, 535–
691 543.
- 692 Clement, K., Rees, H. and Canver, M. C. (2019) CRISPResso2 provides accurate and rapid genome
693 editing sequence analysis. *Nature biotechnology* **37**, 215–226.
- 694 Corcobado, T., Cech, T. L., Brandstetter, M., Daxer, A., Hüttler, C., Kudláček, T., Horta Jung, M. and
695 Jung, T. (2020) Decline of European Beech in Austria: Involvement of *Phytophthora* spp. and
696 Contributing Biotic and Abiotic Factors. *Forests* **11**, 895.
- 697 Creutzburg, S. C. A., Wu, W. Y., Mohanraju, P., Swartjes, T., Alkan, F., Gorodkin, J., Staals, R. H. J.
698 and van der Oost, J. (2020) Good guide, bad guide: spacer sequence-dependent cleavage
699 efficiency of Cas12a. *Nucleic acids research* **48**, 3228–3243.
- 700 Cuervo-Alarcon, L., Arend, M., Müller, M., Sperisen, C., Finkeldey, R. and Krutovsky, K. V. (2018)
701 Genetic variation and signatures of natural selection in populations of European beech (*Fagus*
702 *sylvatica* L.) along precipitation gradients. *Tree Genetics & Genomes* **14**.
- 703 Dai, X., Yang, X., Wang, C., Fan, Y., Xin, S., Hua, Y., Wang, K. and Huang, H. (2021) CRISPR/Cas9-
704 mediated genome editing in *Hevea brasiliensis*. *Industrial Crops and Products* **164**, 113418.
- 705 Das, I. S., Shi, Q., Dreischhoff, S. and Polle, A. (2025) Divergent functions of three Kunitz trypsin
706 inhibitor (KTI) proteins in herbivore defense in poplar. *BMC plant biology*.
- 707 Fan, D., Liu, T., Li, C., Jiao, B., Li, S., Hou, Y. and Luo, K. (2015) Efficient CRISPR/Cas9-mediated
708 Targeted Mutagenesis in Populus in the First Generation. *Scientific reports* **5**, 12217.
- 709 Felton, A., Lindbladh, M., Brunet, J. and Fritz, Ö. (2010) Replacing coniferous monocultures with
710 mixed-species production stands: An assessment of the potential benefits for forest biodiversity in
711 northern Europe. *Forest Ecology and Management* **260**, 939–947.
- 712 Folling, M., Pedersen, C. and Olesen, A. (1998) Reduction of nuclease activity from *Lolium*
713 protoplasts: effect on transformation frequency. *Plant Science* **1**, 29–40.
- 714 Fuchs, Z., Vacek, Z., Vacek, S., Cukor, J., Šimůnek, V., Štefančík, I., Brabec, P. and Králíček, I. (2024)
715 European beech (*Fagus sylvatica* L.): A promising candidate for future forest ecosystems in
716 Central Europe amid climate change. *Central European Forestry Journal* **70**, 62–76.
- 717 Gao, J., Wang, G., Ma, S., Xie, X., Wu, X., Zhang, X., Wu, Y., Zhao, P. and Xia, Q. (2015)
718 CRISPR/Cas9-mediated targeted mutagenesis in *Nicotiana tabacum*. *Plant molecular biology* **87**,
719 99–110.
- 720 García-Plazaola, J. I., Fernández-Marín, B., Ferrio, J. P., Alday, J. G., Hoch, G., Landais, D., Milcu, A.,
721 Tissue, D. T., Voltas, J., Gessler, A., Roy, J. and Resco de Dios, V. (2017) Endogenous circadian

- 722 rhythms in pigment composition induce changes in photochemical efficiency in plant canopies.
723 *Plant, cell & environment* **40**, 1153–1162.
- 724 Gülz, P.-G., Prasad, R., B., N. and Müller, E. (1992) Surface Structures and Chemical Composition of
725 Epicuticular Waxes during Leaf Development of *Fagus sylvatica* L. *Zeitschrift für Naturforschung*
726 **47c**, 190–196.
- 727 Han, X., Rong, H., Feng, Y., Xin, Y., Luan, X., Zhou, Q., Xu, M. and Xu, L.-A. (2023) Protoplast
728 isolation and transient transformation system for *Ginkgo biloba* L. *Frontiers in plant science* **14**,
729 1145754.
- 730 Hirschberg, J. (2001) Carotenoid biosynthesis in flowering plants. *Current Opinion in Plant Biology* **4**,
731 210–218.
- 732 Hong, K., Chen, Z., Radani, Y., Zheng, R., Zheng, X., Li, Y., Chen, J. and Yang, L. (2023)
733 Establishment of PEG-Mediated Transient Gene Expression in Protoplasts Isolated from the Callus
734 of *Cunninghamia lanceolata*. *Forests* **14**, 1168.
- 735 Horstmann, V., Huether, C. M., Jost, W., Reski, R. and Decker, E. L. (2004) Quantitative promoter
736 analysis in *Physcomitrella patens*: a set of plant vectors activating gene expression within three
737 orders of magnitude. *BMC biotechnology* **4**, 13.
- 738 Houston Durrant, T., de Rigo, D. and Caudullo, G. (2016) *Fagus sylvatica* and other beeches in
739 Europe: distribution, habitat, usage and threats. In: *European atlas of forest tree species* (San-
740 Miguel-Ayanz, J., de Rigo, D., Caudullo, G., Houston Durrant, T. and Mauri, A., eds), pp. 94–95.
741 Luxembourg: Publ. Off. EU.
- 742 Hsueh, Y.-W., Chen, M.-T., Patty, P. J., Code, C., Cheng, J., Frisken, B. J., Zuckermann, M. and
743 Thewalt, J. (2007) Ergosterol in POPC membranes: physical properties and comparison with
744 structurally similar sterols. *Biophysical journal* **92**, 1606–1615.
- 745 Huo, A., Chen, Z., Wang, P., Yang, L., Wang, G., Wang, D., Liao, S., Cheng, T., Chen, J. and Shi, J.
746 (2017) Establishment of transient gene expression systems in protoplasts from *Liriodendron* hybrid
747 mesophyll cells. *PLoS one* **12**, e0172475.
- 748 Jia, H., Wang, Y., Su, H., Huang, X. and Wang, N. (2022) LbCas12a-D156R Efficiently Edits *LOB1*
749 Effector Binding Elements to Generate Canker-Resistant Citrus Plants. *Cells* **11**.
- 750 Jinek, M., Chylinski, K., Fonfara, I., Hauer, M., Doudna, J. A. and Charpentier, E. (2012) A
751 programmable dual-RNA-guided DNA endonuclease in adaptive bacterial immunity. *Science* **337**,
752 816–821.
- 753 Keskitalo, M. (2001) Can protoplast production from *in vitro* cultured shoots of *Tanacetum* vary during
754 the season? **10**, 145–151.
- 755 Kim, D., Kim, J., Hur, J. K., Been, K. W., Yoon, S.-H. and Kim, J.-S. (2016) Genome-wide analysis
756 reveals specificities of Cpf1 endonucleases in human cells. *Nature biotechnology* **34**, 863–868.
- 757 Kinraide, T. B. and Wang, P. (2010) The surface charge density of plant cell membranes (σ): an
758 attempt to resolve conflicting values for intrinsic σ . *Journal of experimental botany* **61**, 2507–
759 2518.

- 760 Kishi-Kaboshi, M., Aida, R. and Sasaki, K. (2019) Parsley *ubiquitin* promoter displays higher activity
761 than the CaMV 35S promoter and the chrysanthemum *actin 2* promoter for productive, constitutive,
762 and durable expression of a transgene in *Chrysanthemum morifolium*. *Breeding science* **69**, 536–
763 544.
- 764 Kuzminsky, E., Meschini, R., Terzoli, S., Pavani, L., Silvestri, C., Choury, Z. and Scarascia-Mugnozza,
765 G. (2016) Isolation of Mesophyll Protoplasts from Mediterranean Woody Plants for the Study of
766 DNA Integrity under Abiotic Stress. *Frontiers in plant science* **7**, 1168.
- 767 Lang, H. and Kohlenbach, H. W. (1988) Callus formation from mesophyll protoplasts of *Fagus*
768 *sylvatica* L. *Plant Cell Reports* **7**, 485–488.
- 769 Langer, G. J. and Bußkamp, J. (2023) Vitality loss of beech: a serious threat to *Fagus sylvatica* in
770 Germany in the context of global warming. *J Plant Dis Prot* **130**, 1101–1115.
- 771 Lei, S., Zhu, Y., Jia, W., Zhang, J., Chi, Y. and Xu, B. (2024) A protoplast-based transient gene
772 expression assay for the identification of heat and oxidative stress-regulatory genes in perennial
773 ryegrass. *Plant methods* **20**, 67.
- 774 Letunic, I., Khedkar, S. and Bork, P. (2021) SMART: recent updates, new developments and status in
775 2020. *Nucleic acids research* **49**, D458–D460.
- 776 Li, G., Zhang, Y., Dailey, M. and Qi, Y. (2023) Hs1Cas12a and Ev1Cas12a confer efficient genome
777 editing in plants. *Frontiers in genome editing* **5**, 1251903.
- 778 Li, X., Jiang, D.-H., Yong, K. and Zhang, D.-B. (2007) Varied Transcriptional Efficiencies of Multiple
779 *Arabidopsis U6* Small Nuclear RNA Genes. *JIPB* **49**, 222–229.
- 780 Lorenz, R., Bernhart, S., H., zu Siederdissen, C., H., Tafer, H., Flamm, C. and Stadler, P., F. (2011)
781 ViennaRNA Package 2.0. *Algorithms for Molecular Biology* **6**, 26.
- 782 Lu, H., Zhang, H., Wang, P., Chen, M., Liang, R., Tian, X., Yan, J., Zhan, Y., Xin, Y. and Zeng, F. (2025)
783 Development of a xylem protoplast expression system for gene function analysis and genome
784 editing in *Fraxinus mandshurica* Rupr. *Industrial Crops and Products* **225**, 120446.
- 785 Ma, G., Yan, F., Ren, B., Lu, Z., Xu, H., Wu, F., Li, S., Wang, D., Zhou, X. and Zhou, H. (2024)
786 LbCas12a-nuclease-mediated tiling deletion for large-scale targeted editing of non-coding regions
787 in rice. *Plant communications* **5**, 100815.
- 788 Malzahn, A. A., Tang, X., Lee, K., Ren, Q., Sretenovic, S., Zhang, Y., Chen, H., Kang, M., Bao, Y.,
789 Zheng, X., Deng, K., Zhang, T., Salcedo, V., Wang, K., Zhang, Y. and Qi, Y. (2019) Application of
790 CRISPR-Cas12a temperature sensitivity for improved genome editing in rice, maize, and
791 *Arabidopsis*. *BMC biology* **17**, 9.
- 792 Mao, Y., Zhang, H., Xu, N., Zhang, B., Gou, F. and Zhu, J.-K. (2013) Application of the CRISPR-Cas
793 system for efficient genome engineering in plants. *Molecular plant* **6**, 2008–2011.
- 794 Marillonnet, S. and Grützner, R. (2020) Synthetic DNA Assembly Using Golden Gate Cloning and the
795 Hierarchical Modular Cloning Pipeline. *Current protocols in molecular biology* **130**, e115.

- 796 Marques, B. M., Sulis, D. B., Suarez, B., Yang, C., Cofre-Vega, C., Thomas, R. D., Whitehill, J. G. A.,
797 Whetten, R. W., Barrangou, R. and Wang, J. P. (2025) A Protoplast System for CRISPR-Cas
798 Ribonucleoprotein Delivery in *Pinus taeda* and *Abies fraseri*. *Plants* **14**, 996.
- 799 Masani, M. Y. A., Noll, G. A., Parveez, G. K. A., Sambanthamurthi, R. and Prüfer, D. (2014) Efficient
800 transformation of oil palm protoplasts by PEG-mediated transfection and DNA microinjection. *PLoS*
801 *one* **9**, e96831.
- 802 Merker, L., Schindele, P., Huang, T.-K., Wolter, F. and Puchta, H. (2020) Enhancing *in planta* gene
803 targeting efficiencies in Arabidopsis using temperature-tolerant CRISPR/LbCas12a. *Plant*
804 *biotechnology journal* **18**, 2382–2384.
- 805 Merzlyak, E. M., Goedhart, J., Shcherbo, D., Bulina, M. E., Shcheglov, A. S., Fradkov, A. F., Gaintzeva,
806 A., Lukyanov, K. A., Lukyanov, S., Gadella, T. W. J. and Chudakov, D. M. (2007) Bright monomeric
807 red fluorescent protein with an extended fluorescence lifetime. *Nature methods* **4**, 555–557.
- 808 Mishra, B., Ulaszewski, B., Meger, J., Aury, J.-M., Bodénès, C., Lesur-Kupin, I., Pfenninger, M., Da
809 Silva, C., Gupta, D. K., Guichoux, E., Heer, K., Lalanne, C., Labadie, K., Opgenoorth, L., Ploch, S.,
810 Le Provost, G., Salse, J., Scotti, I., Wötzel, S., Plomion, C., Burczyk, J. and Thines, M. (2021) A
811 Chromosome-Level Genome Assembly of the European Beech (*Fagus sylvatica*) Reveals
812 Anomalies for Organelle DNA Integration, Repeat Content and Distribution of SNPs. *Frontiers in*
813 *genetics* **12**, 691058.
- 814 Naim, F., Shand, K., Hayashi, S., O'Brien, M., McGree, J., Johnson, A. A. T., Dugdale, B. and
815 Waterhouse, P. M. (2020) Are the current gRNA ranking prediction algorithms useful for genome
816 editing in plants? *PLoS one* **15**, e0227994.
- 817 Neubauer, A., Ruaud, S., Waller, M., Frangedakis, E., Li, F.-W., Nötzold, S. I., Wicke, S., Bailly, A. and
818 Szövényi, P. (2022) Step-by-step protocol for the isolation and transient transformation of hornwort
819 protoplasts. *Applications in plant sciences* **10**, e11456.
- 820 Nguyen, L. T., Macaluso, N. C., Rakestraw, N. R., Carman, D. R., Pizzano, B. L. M., Hautamaki, R. C.,
821 Rananaware, S. R., Roberts, I. E. and Jain, P. K. (2024) Harnessing noncanonical crRNAs to
822 improve functionality of Cas12a orthologs. *Cell reports* **43**, 113777.
- 823 Ni, M., CuP, D., Einstein, J., Nerasimhulu, S., Vergara, C. E. and Gelvin, S. B. (1995) Strength and
824 tissue specificity of chimeric promoters derived from the octopine and mannopine synthase genes.
825 *The Plant Journal* **7**, 661–676.
- 826 Nietsch, J., Brüggmann, T., Becker, D. and Fladung, M. (2017) Old methods rediscovered: application
827 and improvement of two direct transformation methods to hybrid poplar (*Populus tremula* × *P.*
828 *alba*). *Plant Cell Tiss Organ Cult* **130**, 183–196.
- 829 Panda, D., Karmakar, S., Dash, M., Tripathy, S. K., Das, P., Banerjee, S., Qi, Y., Samantaray, S.,
830 Mohapatra, P. K., Baig, M. J. and Molla, K. A. (2024) Optimized protoplast isolation and
831 transfection with a breakpoint: accelerating Cas9/sgRNA cleavage efficiency validation in monocot
832 and dicot. *aBIOTECH* **5**, 151–168.

- 833 Pavese, V., Moglia, A., Corredoira, E., Martínez, M. T., Torello Marinoni, D. and Botta, R. (2021) First
834 Report of CRISPR/Cas9 Gene Editing in *Castanea sativa* Mill. *Frontiers in plant science* **12**,
835 728516.
- 836 Pavese, V., Moglia, A., Milani, A. M., Marino, L. A., Martinez, M. T., Torello Marinoni, D., Botta, R. and
837 Corredoira, E. (2024) Advances in *Quercus ilex* L. breeding: the CRISPR/Cas9 technology via
838 ribonucleoproteins. *Frontiers in plant science* **15**, 1323390.
- 839 Pfenninger, M., Reuss, F., Kiebler, A., Schönnenbeck, P., Caliendo, C., Gerber, S., Cocchiararo, B.,
840 Reuter, S., Blüthgen, N., Mody, K., Mishra, B., Bálint, M., Thines, M. and Feldmeyer, B. (2021)
841 Genomic basis for drought resistance in European beech forests threatened by climate change.
842 *eLife* **10**.
- 843 Reed, K. M. and Bargmann, B. O. R. (2021) Protoplast Regeneration and Its Use in New Plant
844 Breeding Technologies. *Frontiers in genome editing* **3**, 734951.
- 845 Sagarbarria, M. G. S., Caraan, J. A. M. and Layos, A. J. G. (2023) Usefulness of current sgRNA
846 design guidelines and in vitro cleavage assays for plant CRISPR/Cas genome editing: a case
847 targeting the polyphenol oxidase gene family in eggplant (*Solanum melongena* L.). *Transgenic*
848 *research* **32**, 561–573.
- 849 Schindele, P. and Puchta, H. (2020) Engineering CRISPR/LbCas12a for highly efficient, temperature-
850 tolerant plant gene editing. *Plant biotechnology journal* **18**, 1118–1120.
- 851 Schindelin, J., Arganda-Carreras, I., Frise, E., Kaynig, V., Longair, M., Pietzsch, T., Preibisch, S.,
852 Rueden, C., Saalfeld, S., Schmid, B., Tinevez, J.-Y., White, D. J., Hartenstein, V., Eliceiri, K.,
853 Tomancak, P. and Cardona, A. (2012) Fiji: an open-source platform for biological-image analysis.
854 *Nature methods* **9**, 676–682.
- 855 Shan, Q., Wang, Y., Li, J., Zhang, Y., Chen, K., Liang, Z., Zhang, K., Liu, J., Xi, J. J., Qiu, J.-L. and
856 Gao, C. (2013) Targeted genome modification of crop plants using a CRISPR-Cas system. *Nature*
857 *biotechnology* **31**, 686–688.
- 858 Stemmer, M., Thumberger, T., Del Sol Keyer, M., Wittbrodt, J. and Mateo, J. L. (2015) CCTop: An
859 Intuitive, Flexible and Reliable CRISPR/Cas9 Target Prediction Tool. *PLoS one* **10**, e0124633.
- 860 Sulis, D. B., Jiang, X., Yang, C., Marques, B. M., Matthews, M. L., Miller, Z., Lan, K., Cofre-Vega, C.,
861 Liu, B., Sun, R., Sederoff, H., Bing, R. G., Sun, X., Williams, C. M., Jameel, H., Phillips, R., Chang,
862 H.-M., Peszlen, I., Huang, Y.-Y., Li, W., Kelly, R. M., Sederoff, R. R., Chiang, V. L., Barrangou, R.
863 and Wang, J. P. (2023) Multiplex CRISPR editing of wood for sustainable fiber production. *Science*
864 **381**, 216–221.
- 865 Tan, B., Xu, M., Chen, Y. and Huang, M. (2013) Transient expression for functional gene analysis
866 using *Populus* protoplasts. *Plant Cell Tiss Organ Cult* **114**, 11–18.
- 867 te Welscher, Y. M., Napel, H. H. ten, Balagué, M. M., Souza, C. M., Riezman, H., Kruijff, B. de and
868 Breukink, E. (2008) Natamycin blocks fungal growth by binding specifically to ergosterol without
869 permeabilizing the membrane. *The Journal of biological chemistry* **283**, 6393–6401.

- 870 Thiesen, F. N., Chmielarz, P., Pawłowski, T. A. and Bubner, B. (2025) Stable in vitro propagation of
871 *Fagus sylvatica* using micro-cuttings established from seedlings. *Plant Cell Tiss Organ Cult* **163**.
- 872 Tuncel, A., Kim, H. U. and Kim, M. C. (2025) Editorial: Engineering future crops through genome
873 editing. *Frontiers in plant science* **16**, 1720325.
- 874 Verosloff, M. S., Corcoran, W. K., Dolberg, T. B., Bushhouse, D. Z., Leonard, J. N. and Lucks, J. B.
875 (2021) RNA Sequence and Structure Determinants of Pol III Transcriptional Termination in Human
876 Cells. *Journal of molecular biology* **433**, 166978.
- 877 Walawage, S. L., Zaini, P. A., Mubarik, M. S., Martinelli, F., Balan, B., Caruso, T., Leslie, C. A. and
878 Dandekar, A. M. (2019) Deploying Genome Editing Tools for Dissecting the Biology of Nut Trees.
879 *Front. Sustain. Food Syst.* **3**, 100.
- 880 Wang, M., Mao, Y., Lu, Y., Tao, X. and Zhu, J.-K. (2017) Multiplex Gene Editing in Rice Using the
881 CRISPR-Cpf1 System. *Molecular plant* **10**, 1011–1013.
- 882 Wang, P., Si, H., Li, C., Xu, Z., Guo, H., Jin, S. and Cheng, H. (2025) Plant genetic transformation:
883 achievements, current status and future prospects. *Plant biotechnology journal* **23**, 2034–2058.
- 884 Wang, X., Xu, L., Liu, X., Xin, L., Wu, S. and Chen, X. (2021) Development of potent promoters that
885 drive the efficient expression of genes in apple protoplasts. *Horticulture research* **8**, 211.
- 886 Weigel, H.-J. (1983) The effect of high temperatures on leaf cells of *Valerianella*: relative heat stability
887 of the tonoplast membrane of mesophyll vacuoles. *Planta* **159**, 398–403.
- 888 Wolabu, T. W., Park, J.-J., Chen, M., Cong, L., Ge, Y., Jiang, Q., Debnath, S., Li, G., Wen, J. and
889 Wang, Z. (2020) Improving the genome editing efficiency of CRISPR/Cas9 in Arabidopsis and
890 *Medicago truncatula*. *Planta* **252**, 15.
- 891 Wühlisch, G. von (2008). *EUFORGEN Technical Guidelines for genetic conservation and use for*
892 *European beech (Fagus sylvatica)*. Rome, Italy.
- 893 Yang, D., Zhao, Y., Liu, Y., Han, F. and Li, Z. (2022) A high-efficiency PEG-Ca²⁺-mediated transient
894 transformation system for broccoli protoplasts. *Frontiers in plant science* **13**, 1081321.
- 895 Yang, P., Sun, Y., Sun, X., Li, Y. and Wang, L. (2024) Optimization of preparation and transformation of
896 protoplasts from *Populus simonii* × *P. nigra* leaves and subcellular localization of the major latex
897 protein 328 (MLP328). *Plant methods* **20**, 3.
- 898 Ye, S., Ding, W., Bai, W., Lu, J., Zhou, L., Ma, X. and Zhu, Q. (2023) Application of a novel strong
899 promoter from Chinese fir (*Cunninghamia lanceolata*) in the CRISPR/Cas mediated genome
900 editing of its protoplasts and transgenesis of rice and poplar. *Frontiers in plant science* **14**,
901 1179394.
- 902 Yoo, S.-D., Cho, Y.-H. and Sheen, J. (2007) *Arabidopsis* mesophyll protoplasts: a versatile cell system
903 for transient gene expression analysis. *Nature protocols* **2**, 1565–1572.
- 904 Zahn, V., Fendel, A., Sievers, A.-J., Fladung, M. and Bruegmann, T. (2025) Benefiting from the past:
905 establishing in vitro culture of European beech (*Fagus sylvatica* L.) from provenance trial trees and
906 seedlings. *Plant methods* **21**, 31.

- 907 Zetsche, B., Gootenberg, J. S., Abudayyeh, O. O., Slaymaker, I. M., Makarova, K. S., Essletzbichler,
908 P., Volz, S. E., Joung, J., van der Oost, J., Regev, A., Koonin, E. V. and Zhang, F. (2015) Cpf1 is a
909 single RNA-guided endonuclease of a class 2 CRISPR-Cas system. *Cell* **163**, 759–771.
- 910 Zhang, L., Li, G., Zhang, Y., Cheng, Y., Roberts, N., Glenn, S. E., DeZwaan-McCabe, D., Rube, H. T.,
911 Manthey, J., Coleman, G., Vakulskas, C. A. and Qi, Y. (2023) Boosting genome editing efficiency in
912 human cells and plants with novel LbCas12a variants. *Genome biology* **24**, 102.
- 913 Zhang, X., Wang, L., He, C. and Luo, H. (2016) An efficient transient mesophyll protoplast system for
914 investigation of the innate immunity responses in the rubber tree (*Hevea brasiliensis*). *Plant Cell*
915 *Tiss Organ Cult* **126**, 281–290.
- 916 Zhao, X., Song, H., Liu, J., Feng, K., Wu, Q., Arif, T., Cao, Y. and Zhang, L. (2025) Efficient Protoplast
917 Isolation and PEG-mediated Transformation protocols for blueberry *Vaccinium corymbosum*.
918 *Scientia Horticulturae* **340**, 113916.
- 919 Zhou, H., Lei, Y., Hou, Z., Yuan, J. and He, N. (2024a) Efficient mesophyll-derived protoplast
920 manipulation system as a versatile tool for characterization of genes responding to multiple stimuli
921 in mulberry. *Plant Cell Tiss Organ Cult* **156**.
- 922 Zhou, H., Song, X. and Lu, M.-Z. (2024b) Growth-regulating factor 15-mediated vascular cambium
923 differentiation positively regulates wood formation in hybrid poplar (*Populus alba* × *P. glandulosa*).
924 *Frontiers in plant science* **15**, 1343312.
- 925 Zhu, H. and Liang, C. (2019) CRISPR-DT: designing gRNAs for the CRISPR-Cpf1 system with
926 improved target efficiency and specificity. *Sequence analysis* **35**, 2783–2789.
- 927